Contract Report

High Throughput, Low Toxic Processing of Very Thin, High Efficiency CIGSS Solar Cells

NREL contract no. XXL-5-44205-08, UCF/FSEC Account no. 2012 8098

Year 1, Annual Report

Report no. FSEC-CR-1637-06

July 06, 2006

Prepared for

National Renewable Energy Laboratory
1617 Cole Boulevard
Golden, CO 80401

Submitted by

Neelkanth G. Dhere
Florida Solar Energy Center®
1679 Clearlake Road
Cocoa, FL 32922-5703

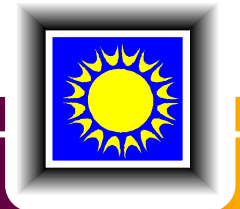

TABLE OF CONTENTS

LIST OF FIGURES

LIST OF TABLES

LIST OF ACRONYMS/ABBREVIATIONS

V_{oc}	: Open Circuit Voltage
J_{sc}	: Short circuit current density
FF	: Fill Factor
R_{sh}	: Shunt Resistance
R_s	: Series Resistance
I_{pk}	: Peak current
V_{pk}	: Peak Volatge
I-V	: Current-Voltage
QE	: Quantum Efficiency
η	: Efficiency

1: INTRODUCTION

Copper indium diselenide, $CuInSe_2$ (CIS), is an excellent absorber material for the development of highly efficient and low-cost thin film solar cell devices due to its high absorption coefficient and near optimal bandgap value. The incorporation of gallium ($CuIn_{1-x}Ga_xSe_2$, CIGS) is known to enhance the range over which the chalcopyrite phase α is formed. Moreover, the addition and sulfur ($CuIn_{1-x}Ga_xSe_{2-y}S_y$, CIGSeS) has been used to produce graded bandgap structures in order to further increase the efficiency of devices by obtaining a higher charge carrier collection. The present highest cell efficiencies of CIGS cells and CIGSeS module are 19.5% and 13.1% respectively [1, [2].

Many recent presentations and publications from Linda L. Horton, Oak Ridge National Laboratory, Richard Smalley, Rice University and Nathan Lewis, California Institute of Technology, have emphasized that among the renewables, only solar energy has the resource to make a substantial contribution to non-CO_2 energy in the 21st century. The rest of the renewable options (wind, biomass, geothermal, hydro) do not have adequate global resources to do more than fill in for solar when solar is unavailable – although such "filling in" may be about a Terawatt each (still a very significant contribution). This means that solar (with about 125,000 TW of global incident energy) has both a huge opportunity and a huge responsibility [3[6].

The mid-term goal of the photovoltaic industry is to develop technology to reduce the manufacturing cost to below $1/peak watt to make the technology competitive with some of high end applications. The research activities of the FSEC PV Materials Lab are focused on developing scalable processes for economic, large-scale manufacture of CIGSeS thin film solar cells.

Thin film solar cells use a direct bandgap semiconductor such as CIGSeS and CdTe with very high absorption coefficient so that most of the sunlight can be absorbed in a layer of less than even1 micron thick with the mass per unit area of semiconductor of approximately 3-6 g/m^2, that will provide ~100 W/m^2 at an photovoltaic convenrsion efficiency of 10%. Thus even material cost would only be pennies per watt at this level. Among all thin films, CIS based thin films have the highest cell and module efficiencies and to date. Moreover, CIS does not suffer from instrisic degradation mechanisms such as Staebler-Wronski effect. However, with the

recent increase in the cost of indium, the need for thin CIS, CIGS or CIGSeS thin film solar cells has increased.

Indium is a rare metal that commonly occurs as an impurity in zinc and to a lesser extent in tin, lead and copper. The abundance of indium in the earth's crust is believed to be equivalent to the occurrence of silver, however, the similarities end there. Over the last two years cost of indium per kilogram has increased ten times ($60/kg in 2002 to more than $600/kg in 2005) [7].

The availability of indium could become a limiting factor if CIGSeS PV modules were to satisfy a sizable fraction of global energy demand. Indium consumption could be lowered by higher materials utilization, use of thinner films, and substitution by gallium, and higher module efficiencies. Based on the high absorption coefficient of 10^5 cm^{-1} for photon energy above the bandgap, Zweibel [8] estimates that the CIGS thickness can be reduced to 0.5 μm without light-trapping and to 0.2 μm with sophisticated light-trapping. For thinner cells, the collection efficiency would improve because the distance between the space-charge edge and light-generated electron-hole pairs would become smaller compared to the minority-carrier diffusion length. Spitzer et al [9] estimated that efficiencies exceeding 25% should be achievable for single-junction, chalcopyrite-based devices using a 1-μm absorber layer with bandgaps of 1 - 1.5 eV, assuming negligible surface recombination velocity and no absorption in the window material.

Making cells thinner could reduce the time required for deposition and thereby increase the throughput. However, there is a higher probability of photogenerated minority carriers being lost at the back contact in a thinner CIGSeS layer. This can be avoided by adding an adequate amount of gallium that has a tendency to diffuse to the back contact during selenization/sulfurization and thus would create a back-surface field repelling the electron toward the p-n junction. Lundberg et al [10] obtained efficiencies as high as 15% on a 1-μm-thick CIGS absorber layer with back-surface field provided by Ga near the back contact. Below a thickness of 0.8 μm, recombination increased due to absorbance-related losses and poor material quality while short circuit current decreased due to absorbance related losses and reduced carrier collection. Negami et al [11] reported a decrease in open-circuit voltage and fill factor for 0.47-μm-thick CIGS because of shunting paths through CdS formed due to excessive surface roughness. Absorbance as well as shunting-related losses could be reduced by improving the

material quality. Thus there is a formidable but achievable goal of meeting terawatt challenge at a reduced cost and keeping efficiencies up to the mark.

Over the last few years, excellent facilities have been developed at FSEC for the development of p-type CIGSS thin films on large, 10 cm x 15 cm substrates [12[14]. CIGSeS thin films were prepared on glass in two steps. Step one involved the deposition of CuGa-In metallic precursors on molybdenum coated glass substrate using DC magnetron sputtering and step two involved the selenization/sulfurization of these metallic precursors either by using diluted diethylselenide (DESe) as a selenium source and diluted H_2S as a sulfur source respectively, or by rapid thermal processing (RTP) using elemental selenium and diluted H_2S as a sulfur source.

2: OPTIMIZATION OF METALLIC PRECURSOR DEPOSITION AND SELENIZATION/SULFURIZATION IN THE CONVENTIONAL FURNACE

Experiments were carried out to optimize Cu/In+Ga ratio, amount of NaF and the selenization/sulfurization temperature and time. The metallic precursors CuGa and In were deposited by DC magnetron sputtering technique. The Cu/In+Ga ratio was varied from ~ 0.7 – 1.05. NaF of up to 12 nm was deposited after the deposition of metallic precursor by thermal evaporation. The selenization of the precursor was carried out at various temperatures raging from 400 °C to 525°C and time raging from 10 minutes to 85 minutes. The sulfurization temperature was carried out at the highest selenization temperature and the time varied from 10 min to 30 min. Comparative analysis between the etched and unetched absorber layers was also carried out.

Addition of sodium improved the grain size as well as the grains were faceted. It also improved the conductivity of the film. The highest cell efficiency obtained was 6.12%.

Experiments were carried out to determine the optimum selenization temperature and soaking time at that temperature. The metallic precursors CuGa and In were deposited using DC magnetron sputtering technique. In the earlier experiments NaF was added after the deposition of CuGa and In metallic precursors. Afterwards realizing that Na also plays a role in enhancing the nucleation during the CIGSeS phase formation **[15]**, NaF was deposited prior to the CuGa and In metallic precursors, a small amount (up to 12 nm) of NaF was deposited to facilitate the crystalline growth of the chalcopyrite crystal [16]. Having achieved some promising results a series of experiments were also carried out on 2 mil (50 μm) polished stainless steel foil.

The completed cells were sent to NREL for current-voltage (I-V) and quantum efficiency measurements. These results are presented and analysed in the following.

Initial optimization of the Cu/(In+Ga) ratio, NaF thickness and selenization temperature, resulted in an efficiency of 12.33% as shown in the Figure 1a. The cells were completed by deposition of CdS heterojuction partner layer by chemical bath deposition followed by i:ZnO/ZnO:Al transparent and conducting window bilayer by RF magnetron sputtering and finally a Cr/Ag front contact grid through a mechanical mask. The efficiencies of these cells when measured with the I-V setup of PV Material Laboratory were greater than 9%. The same cells were measured at the National Renewable Energy Laboratory and the official confirmed

total-area efficiency was above 12% with highest efficiency of 12.33%. The other electrical parameters of the cell were; Voc – 495 mV, Jsc – 39.15 mA/cm2 and FF – 63.53%.

Current versus voltage (I-V) (Figure 1a) and quantum efficiency (QE) curve (Figure 1b) provide valuable information about the cell and potential areas of improvement. The short circuit current density, J_{sc} value of 39.15 mA/cm^2 is near the maximum possible value for CIS with minimum recombination and interface losses. This indicates that the bulk of the material is well selenized with minimum defects. The open circuit voltage, Voc value of 495 mV is low and suggests a potential area of improvement at the p-n junction. The open circuit voltage, V_{oc} can be further improved by three possible ways: 1) Fine tuning the amount of CuGa so as to achieve Cu/(In+Ga) ratio of between 0.88 and 0.92 and thereby reducing the In_{Cu} antisite compensating donors; 2) Increasing the thickness of i:ZnO to prevent shortening and leakage current paths; 3) Optimizing the post-sulfurization parameters to effectively reduce the recombination centers in the space charge region and also to passivate the surface. In order to improve the fill factor, FF the series resistance should be as low as possible while the shunt resistance should be as high as possible. The shunt resistance value was acceptable however, the series resistance needs to be further reduced by optimizing the thickness of ZnO:Al. The fill factor (FF) can be further improved by using Nickel/Aluminum as contact fingers instead of chromium/silver as nickel has better lattice matching with ZnO.

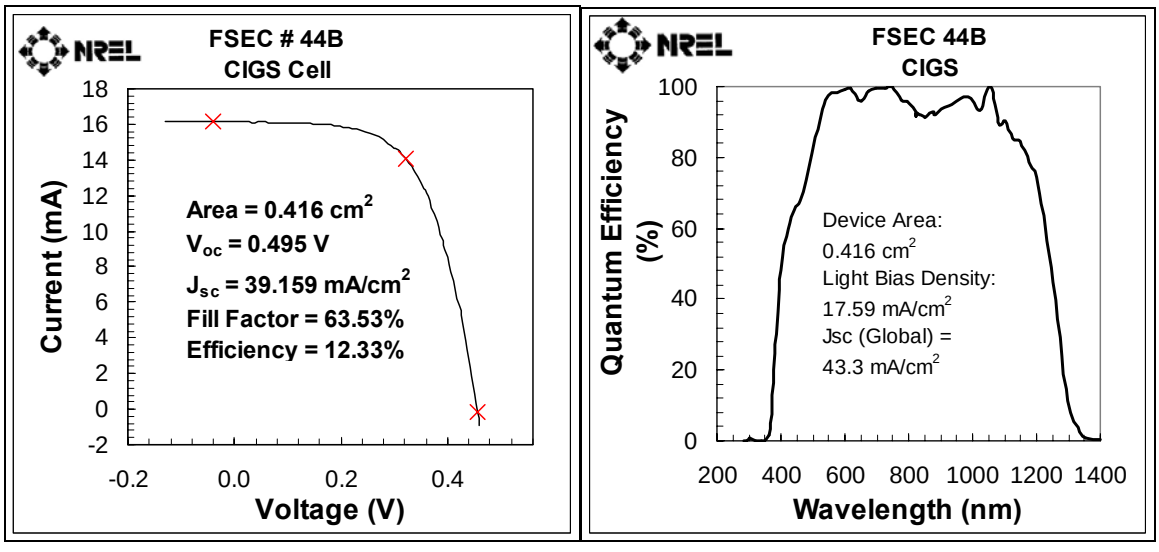

a b

Figure 1: a) Current –voltage characteristics (I-V) and b) QE characteristics of the cell having 8 nm layer of NaF and selenized

Performance of the cells was further improved beyond 13% by selenization/sulfurization treatment and optimizing the i:ZnO thickness. Corresponding current-voltage characteristic and the quantum efficiency of CIGSS/CdS thin film solar cell is shown in figure 3a and 3b respectively. The Voc improved from 495 mV to 540 mV. The highest efficiency of 13.73% was obtained and the corresponding electrical parameters were open circuit voltage, Voc –540 mV, short circuit current density, Jsc –38.37 mA/cm2 and fill factor, FF – 66.33%. The morphology of the films was studied by scanning electron microscopy. The topographic view in figure 2a shows that the grains are highly faceted and have dimension greater than 1 μm. Moreover, the cross-sectional view in figure 2b shows that the grains extend from back contact to the surface. The dip at 800 nm in Quantum Efficiency curve of earlier cell (figure 1b) was not observed in this case as sulfur passivated the recombination centers. The curve was flat in the center region; however noticeable free carrier absorption was still evident. To the best of our knowledge the efficiency of 13.73% is the world record on small area cells prepared by selenization/sulfurization in conventional furnace.

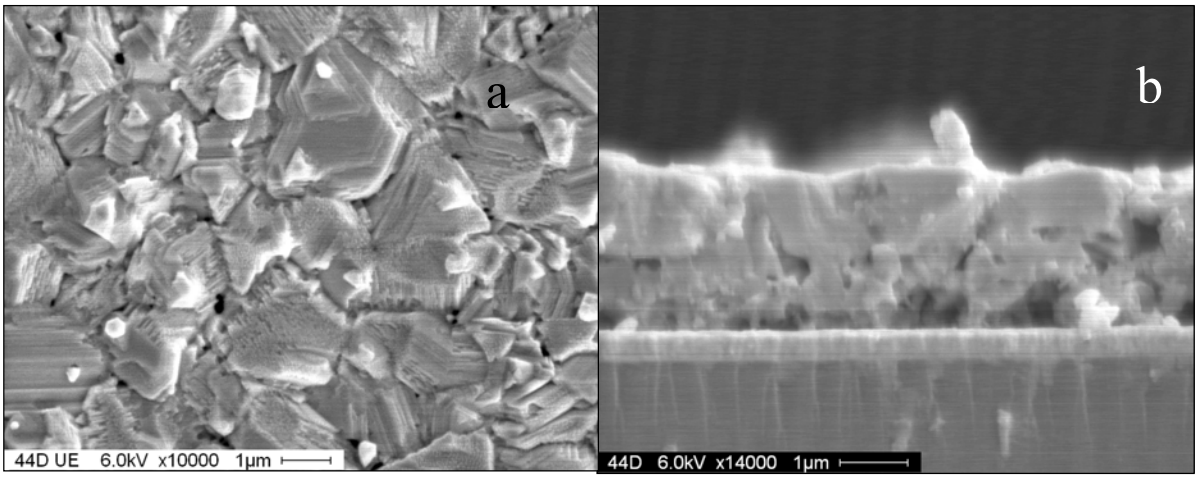

Figure 2: SEM image of the film selenized and sulfurized, a) topographic view at 10000X b) Cross-sectional view at 14,000X

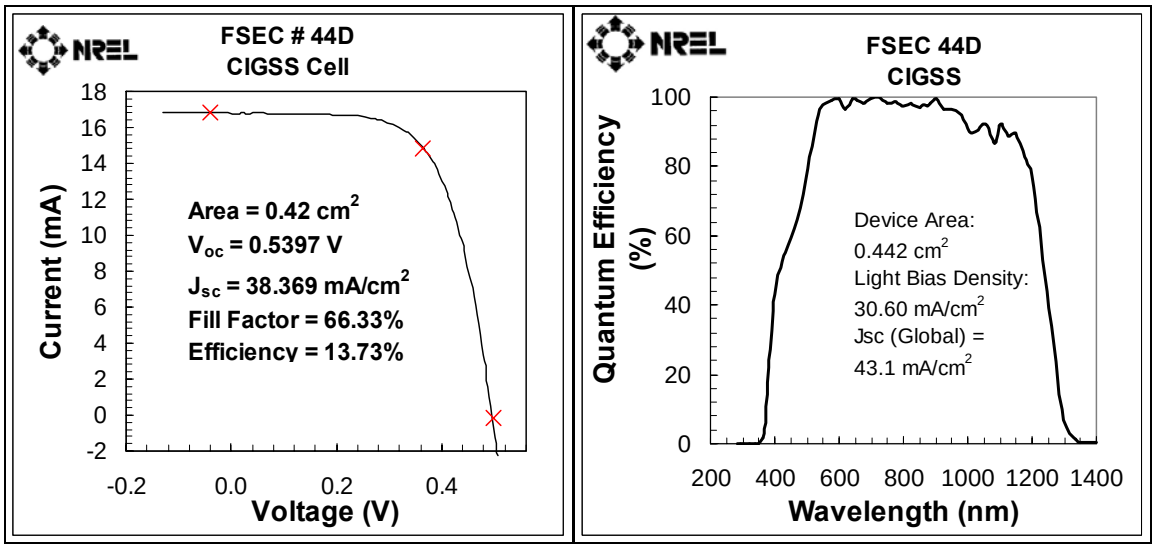

a b

Figure 3: a) Current –voltage characteristics (I-V), b) QE characteristics of the cell having 8 nm layer of NaF and selenized/sulfurized

3: RAPID THERMAL PROCESSING

Rapid thermal processing (RTP) provides a way to rapidly heat substrates to an elevated temperature to perform relatively short duration processes. RTP can be utilized to minimize the process cycle time and the thermal budget without compromising process uniformity, thus eliminating a bottleneck in $CuIn_{1-x}Ga_xSe_{2-y}S_y$ (CIGSeS) module fabrication. Some approaches have been able to realize solar cells with conversion efficiencies close or equal to those for conventionally processed solar cells with similar device structures.

Florida Solar Energy Center (FSEC) PV Materials Lab has developed excellent facilities for the preparation of CIGSS thin-film solar cells. A RTP reactor for preparation of CIGSeS designed, assembled and tested at the FSEC PV Materials Lab. The synthesis and characterization of CIGSeS thin-film solar cells by RTP technique is described in the following.

Several experiments were carried out to optimize the amounts of NaF evaporated on to Mo-cotaed glass substrates prior to the deposition of CuGa, In metallic precursors and of selenium on to CuGa, In metallic precursors for the preparation of CIGSeS thin films by RTP. In initial experiments CIGSeS films peeled off mainly due to overheating. The sample soaking time at process temperature was reduced to reduce overheating. These CIGSeS films did not peel off. The sheet resistance was 100-200 KΩ/□. Moreover, the cell efficiencies were low (~1%).

RTP carried out after initial optimization of the amount of Se resulted in uniform samples that did not peel off. Sheet resistance value of 20-100 Ω/□ was obtained. Samples were sent to NREL for electron probe microanalysis (EPMA) and X-ray diffraction (XRD) analysis.

In continuation of these experiments RTP was carried out. Comparatively lower sheet resistance values of ~ 20-100 Ω/□ were observed and this is mainly attributed to loss of Se during RTP. Selenium quantity was optimized and another set of experiments was carried out.

Auger electron spectroscopy (AES), Secondary Ion Mass Spectroscopy (SIMS), X-ray diffraction (XRD) and electron probe microanalysis (EPMA) analyses were carried out. The results are reported in figure 4, 5, 6.

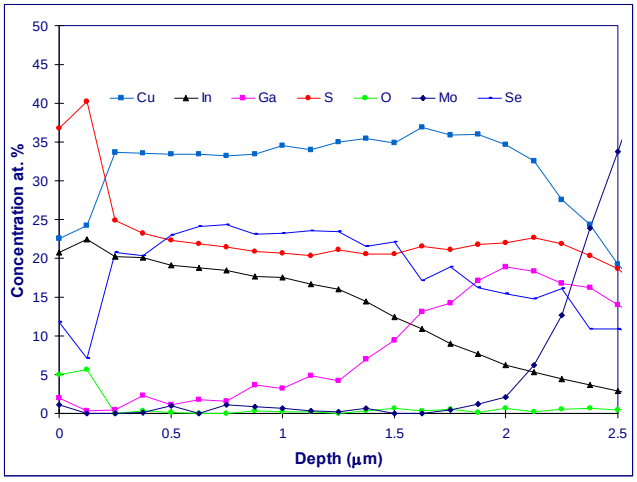

Figure 4: AES depth profile

The depth profile showed that gallium concentration increases towards the back contact while that of indium decreases.

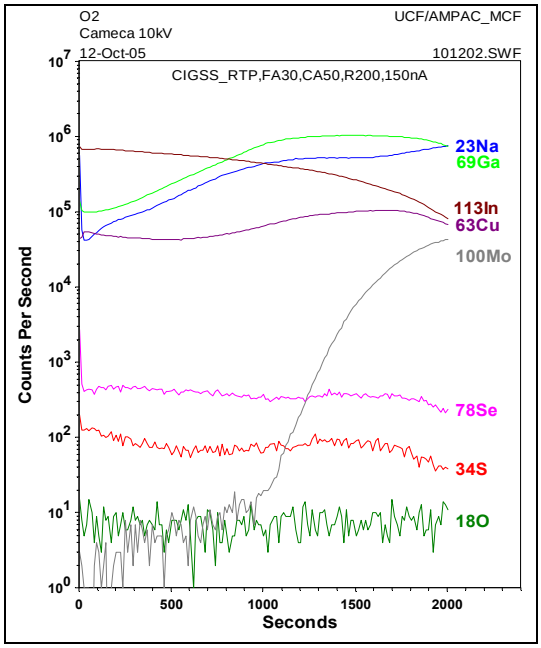

Figure 5: Secondary Ion Mass Spectroscopy analysis

SIMS depth profiling (Figure 5) was performed on an etched sample using a CAMECA system with oxygen primary beam current 150 nA, with source at 10 keV. Ga concentration increased towards the Mo back-contact. Indium concentration decreased near the Mo back-contact. Na was added intentionally.

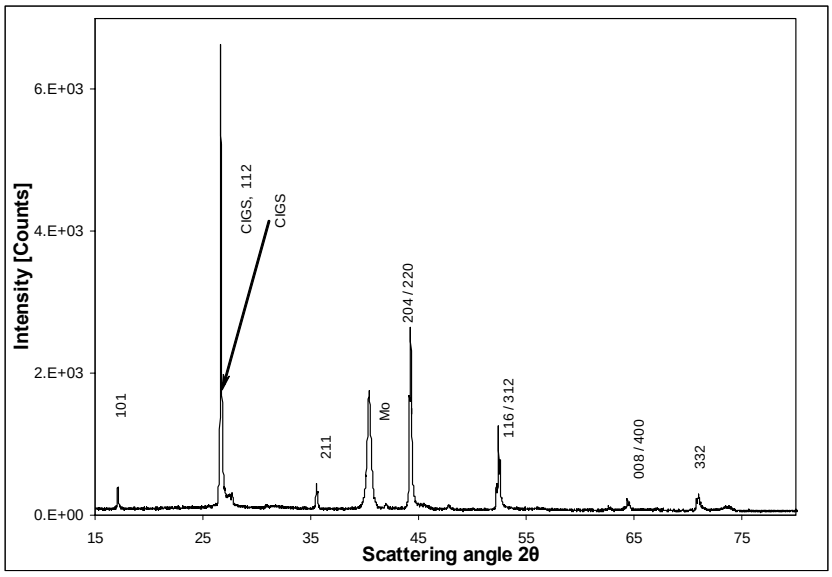

Figure 6: X-ray diffraction pattern

X-ray diffraction (XRD) was used to identify the crystalline phases. The XRD pattern of a near-stoichiometric, slightly Cu-poor, etched CIGSS thin film is shown in figure 6; it showed sharp reflections from chalcopyrite crystal structure (101), (112), (211), (204)/(220), (116)/(312), (008)/(400), and (332). A Mo peak was obtained at 40.22°. The XRD pattern shows a high degree of (112) preferred orientation.

In earlier experiments, the sheet resistance of the sample was observed to be very low. It was suspected that there was an extreme loss of Se in the form of In_2Se_3. Further samples were designed to obtain a Cu/In+ Ga ratio of approximately 0.92. EPMA analysis data of selenized sample is given in TableI.

Table I: EPMA analysis data for selenized sample.
Cu/In+Ga = 0.93

Cu (At%)	In (At%)	Ga (At%)	Se (At%)
24.52	20.55	6.01	24.44

Table II: EPMA analysis data for selenized and sulfurized sample.
Cu/In+Ga = 0.92

Cu (At%)	In (At%)	Ga (At%)	Se (At%)	S (At%)
24.24	19.28	6.92	27.05	22.48

EPMA data (from NREL) for this selenized and sulfurized sample (Table II) showed the ratio S/Se+S of ~20% higher than the optimum of ~10%. Further experiments were designed to optimize the S/Se+S ratio at ~10% (at. wt) [17]. The sheet resistances achieved after rapid thermal processing were around 10KΩ/□. CIGSeS thin-film solar cells were completed by chemical bath deposition of CdS hetrojunction partner layer followed by RF magnetron sputter deposition of i:ZnO/ZnO:Al transparent and conducting oxide window bilayer and then Cr/Ag contact fingers by thermal evaporation. Current-voltage (I-V) characteristics (Figure 7) obtained using the I-V setup that was built in-house showed an improved efficiency of ~4% (Table III).

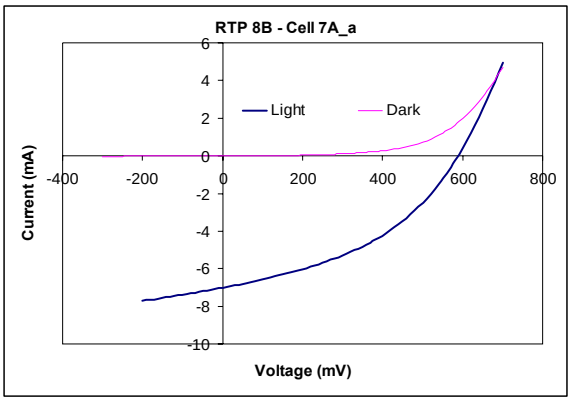

Figure 7: I-V characteristics for CIGSeS solar cell processed by RTP

Table III: Device parameters for the cell processed by RTP

Parameter	Value
Rsh	279.22 Ω
Rs	31.65 Ω
Area	0.441 cm^2
I_{sc}	-7.01 mA
V_{oc}	589.99 mV
I_{pk}	-4.60 mA
V_{pk}	370.00 mV
Fill Factor	41.24 %
Efficiency	3.87 %

In the following experiments, optimization of the RTP process was continued with an increase in the sheet resistance of CIGSeS film increasing from 10kΩ/□ to 1MΩ/□. Films were examined visually for their appearance, color and any tendency to peel. Surface morphology of the CIGSeS thin film was studied using scanning electron microscopy (SEM). Chemical composition was

analyzed by electron probe microanalysis (EPMA). Depth profiling was performed by Auger electron spectroscopy (AES). Thicknesses of thin films were measured using a thickness profilometer. Current–voltage (I-V) characteristics of CIGSeS solar cells were measured under AM 1.5 conditions using a set-up developed at the FSEC PV Materials Lab and then were sent to NREL for I-V and QE analysis.

The SEM image of a near-stoichiometric, slightly Cu-poor, CIGSeS thin film is shown in figure 8a and a cross-sectional SEM image of the same thin film is shown in figure 8b. The sample showed well-faceted grains of approximately 1 µm size.

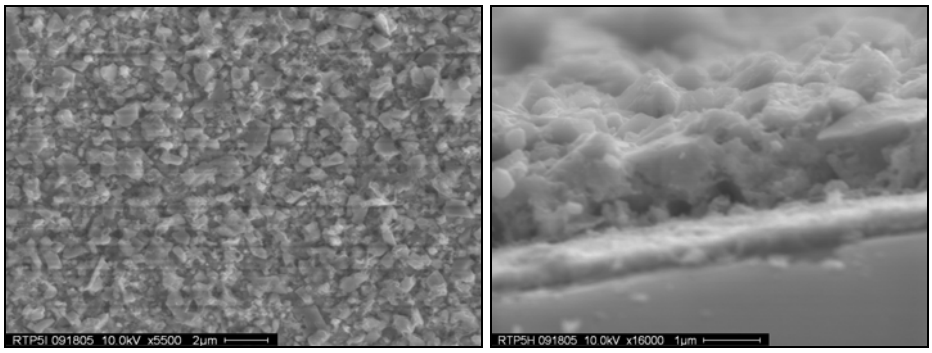

a b

Figure 8: SEM image of a near-stoichiometric, slightly Cu-poor, CIGSeS thin film
a) Topographic view at 5500X b) Cross-sectional view at 16,000X

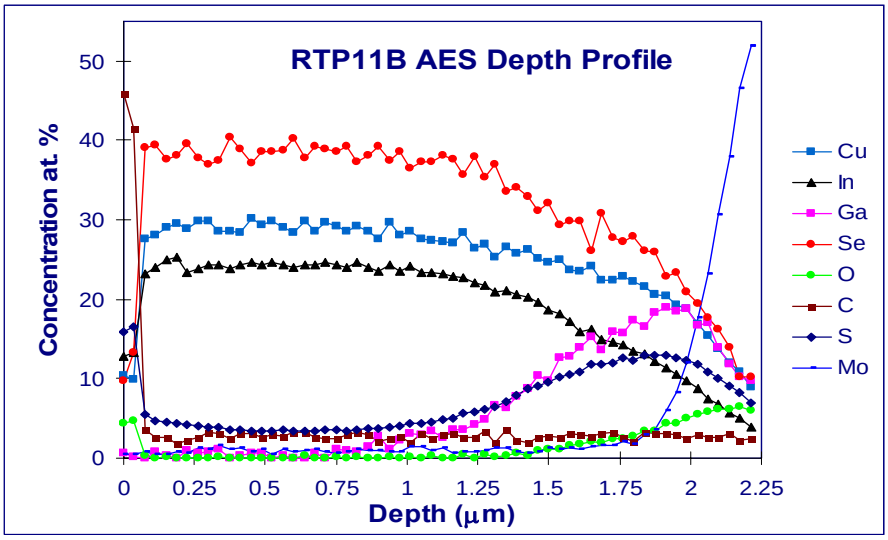

Figure 9: AES depth profile of near-stoichiometric, slightly Cu-poor,CIGSeS thin film

The AES depth profile (Figure9) was obtained by sputtering with energetic argon ions at a rate of 500Å/min. The depth profile showed that gallium concentration increases towards the back contact while that of indium decreases. Also, higher concentration of sulfur was observed near the surface and at the CIGSeS interface and near Mo back contact. Sulfur diffuses through grain boundaries and near Mo back contact the grain size is comparatively smaller so there is more sulfur diffusion towards the back contact. Small grains at Mo interface were also evident in the SEM image (Figure 8). Post sulfurization reduces selenium vacancies and also the recombination centers in the space charge region thereby increasing the $V_{oc.}$ Absorber thickness was measured with the surface profile measuring system and was found to be approximately 2 μm.

Efficiency of CIS improves by bandgap widening at the junction through addition of Ga and S. Gallium improves V_{oc}. However, the concentration of gallium near the surface (where the junction is formed) is very low while it is high near the back contact (Figure 9). The accumulation of Ga at the back creates a back surface field. The back surface field helps in improving solar cell performance. Sulfur is present at the surface and near the back contact. I-V data (figure 10a) shows V_{oc} of 573 mV, through the increase of band gap in the depletion region and the passivation of defects.

The I-V characteristics were measured using a setup built in-house at the FSEC PV Materials Lab as well as at NREL. Some of the I-V and QE analysis are shown here. Presently efficiencies are approaching 13% (total area efficiency) (details are given in figure 10a and 10b. and Table IV).

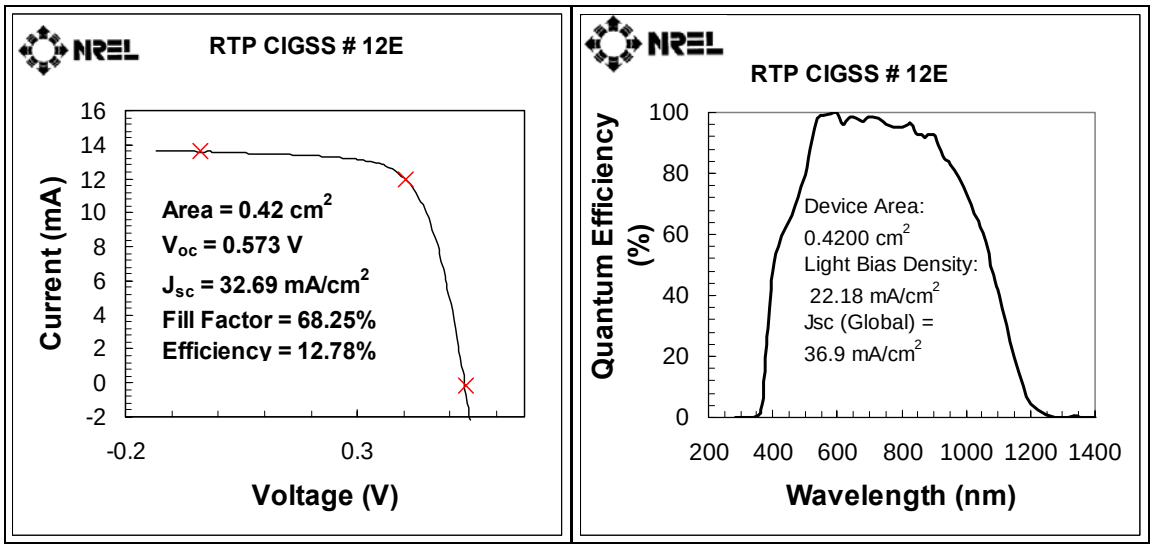

a b

Figure 10: a) I-V and b) QE Characteristics of cell 12E

The improvement in the electrical parameters with optimization of RTP parameters has been summarized in Table IV

Table IV: Improvement in I-V characteristics for CIGSeS thin film solar cells.

Cell #	Voc (mV)	Jsc	FF	%η
10E	545	30.41	65.97	10.93
12E	573	32.69	68.25	12.78
14B	613	33.05	62.97	12.75

Further optimization of the process is being carried out to improve these parameters. Thus during the research carried out so far in this year on rapid thermal processing for the formation of CIGSeS thin film solar cells, encouraging results were obtained and it was demonstrated that reasonable solar cell efficiencies (approaching 13%) can be achieved with relatively shorter cycle times, lower thermal budgets and without using toxic gases such as hydrogen selenide or diethyl selenium for selenization.

4: ULTRA THIN CIGSeS THIN FILM SOLAR CELLS

Detailed study was carried out to understand the necessity of thinner CIGSeS absorber layer through the "Terawatt Challenge" and the indium cost. Initial experiments were carried out to prepare 0.9 μm thick CIGSeS absorber layer. The absorber layer was studied through materials characterization techniques such as scanning electron microscopy (SEM) for morphology, X-ray energy dispersive spectroscopy (XEDS) for composition, secondary ion mass spectroscopy (SIMS) and Auger electron spectroscopy (AES) for depth profile and X-ray diffraction (XRD) to determine the details of crystal structure.

The metallic precursors CuGa and indium were deposited using DC magnetron sputtering technique. The thickness of the metallic precursors was reduced proportionately. Selenization and sequential selenization/sulfurization of these metallic precursors were carried out using the conventional and rapid thermal processing approaches respectively. The cells were completed by deposition of CdS buffer layer using CBD and window bilayer of i:ZnO/Zno:Al by RF magnetron sputtering and then Cr/Ag contact fingers by thermal evaporation. Current-voltage (I-V) characteristics were obtained for these cells using the I-V setup that was built in-house.

Experiments were carried out to determine the optimum parameters for selenization/sulfurization. Different selenization soaking times at maximum process temperature were tried in the conventional furnace. It was observed that the series resistance of the sample reduced with the reduction in soaking time. The possible explanation for this observation was that with higher soaking time the molybdenum layer was affected as most of the molybdenum was converted to $MoSe_2$ layer and therefore, not forming ohmic contacts. Highest efficiency of 6.26% was achieved, as measured at the FSEC, PV Mat Lab Facility.

For the rapid thermal processing approach, experiments were carried out with optimization of the sulfur content. By optimizing the sulfur content in the film, efficiency of 6.58% was achieved, as measured at the FSEC PV Mat Lab Facility. This same sample when measured at NREL showed an efficiency of 8.65%. The current-voltage characteristics and the quantum efficiency curve for this sample are shown in figure 11.

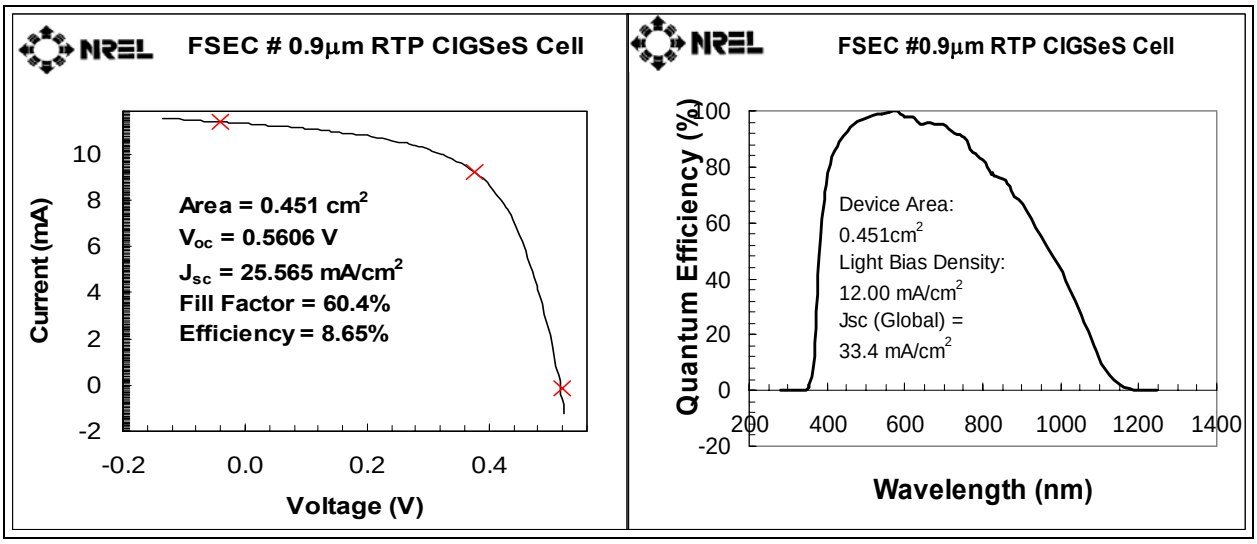

Figure 11: a) I-V and b) QE Characteristics of 0.9 µm RTP CIGSeS cell

The open circuit voltage was measured to be 560 mV which suggests that there was sulfur incorporation into the bulk of the material also the bandgap calculated from the quantum efficiency curve is about 1.13 eV which again suggests the bandgap shift due to sulfur incorporation. The short circuit current density measured using the current-voltage characteristics is 25.565 mA/cm^2. This could be because of poor absorber quality as can be seen from the quantum efficiency curve. The red response shows that the recombination losses are very high due to which the current density is low which suggests poor absorber film material.

For the future, experiments are designed to optimize parameters for selenization/sulfurization in the conventional furnace as well as in the RTP set-up.

5: SULFURIZATION APPROACH FOR LOW TOXIC ABSORBER

$CuIn_{1-x}Ga_xS_2$ (CIGS2) thin films were prepared in two steps. Step one consisted of the deposition of CuGa-In metallic precursors using DC magnetron sputtering. The metallic precursors were deposited in the copper excess composition of Cu/(In+Ga). Step two consisted of sulfurization of metallic precursors in dilute H_2S ambient. Since the CIGS2 growth was carried out in the copper excess composition, excess copper segregated on top of CIGS2 in the form of $Cu_{2-x}S$ was etched away using 10% KCN solution.

XRD pattern of etched CIGS2 thin film shows (101), (112), (103), (200), (220), (312), (400), (316) and (424) reflections of highly crystalline chalcopyrite CIGS2 and also reflections from molybdenum (Figure 12). The strongest reflection was from the (112) plane at $2\theta = 27.92°$. The lattice parameters calculated were a = 5.52 Å and c = 11.04 Å. Molybdenum reflection was observed at $2\theta = 40.4°$. The intensity ratio of I(112)/I(220/204), measured for these films was 2.74, showing a preferred {112} orientation.

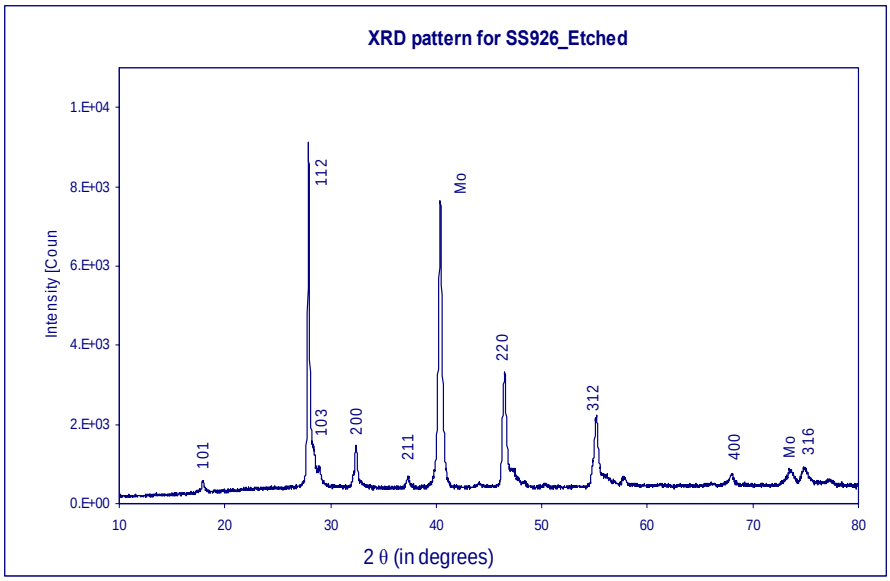

Figure 12: XRD pattern of series cell prepared in Cu/(In+Ga)=1.4 ratio

Figure 13 shows the I-V characteristic of the best cell measured at NREL. Device parameters were V_{oc}, 830.2 mV, J_{sc}, 20.88 mA/cm^2, FF 69.13% and efficiency of 11.99%. This is the world record efficiency to date for selenide-free CIGS2/CdS thin film solar cells prepared by

sulfurization of metallic precursors. The highest efficiency so far on CIGS2/CdS thin film solar cells is 12.3% developed using two stage co-evaporation techniques [18]. The open circuit voltage reported in this research (830.2 mV) is the highest ever obtained on CIGS2/CdS thin-film solar cells. The cells have been awarded the "Voc champions" title.

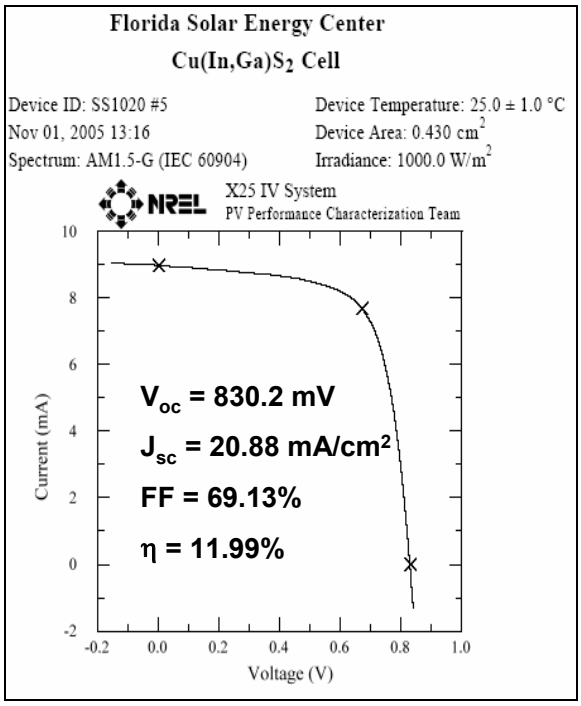

Figure 13: I-V characteristic of the highest reported Voc cell, measured at NREL

TEM analysis

The CIGS2 absorber layer is fairly smooth throughout with occasional waviness. Large-sized CIGS2 grains of about 1 μm size are seen on the top side towards the CdS layer whereas small grains of about 150 nm size are observed close to the Mo back contact (Figure 14). Adhesion between the layers looks good especially that between CIGS2 and Mo. Some porosity is seen in the small-sized CIGS2 grains near the Mo layer in early CIGS2 layers.

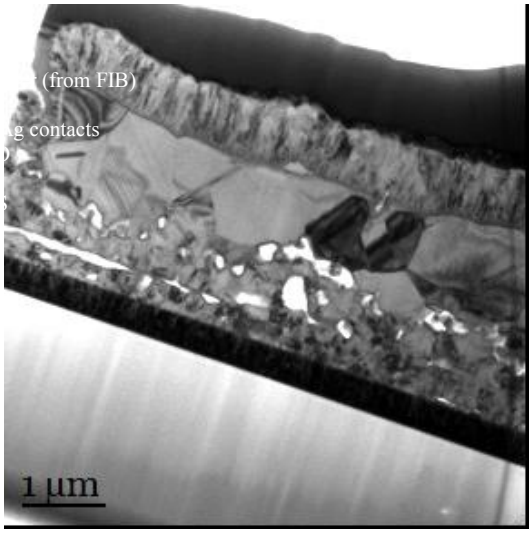

Figure 14: Bright field transmission electron micrograph giving an overview of the cross-section of the CIGS2 –based thin film solar cell

6: ACKNOWLEDGEMENTS

The authors would like to acknowledge the kind help from Dr. Helio Moutinho, Dr. Bobby To, and Dr. Tom Moriarty from NREL for carrying out the XRD, EPMA, and current-voltage (I-V) analysis respectively, Mr. Mikhail Kilmov of AMPAC's Materials Characterization facility (MCF) at UCF for carrying out SIMS analysis and the NREL thin-film PV partnership program for funding this research through contract number XXL-5-44205-08.

7: REFERENCES

[1] Miguel A. Contreras, K. Ramanathan, J. AbuShama, F. Hasoon, D. L. Young, B. Egaas and R. Noufi, Prog. Photovolt: Res. Appl. 2005; 13:209–216.

[2] N. G. Dhere and R. G. Dhere, "Thin-Film Photovoltaics" J. Vac. Sci. & Technol, (A) 23, (2003), pp. 1208-1214.

[3] L. L. Horton, Basic Research Needs to Assure a Secure Energy Future, Workshop on Neutron and Energy for Future, 2004.

[4] R. E. Smalley, Our Energy Challenge, Columbia University NYC September 23, 2003, 31st IEEE PVSC, 2005, Keynote Speech.

[5] N. S. Lewis, Scientific Challenges in the Development of Sustainable Energy, 31st IEEE PVSC, 2005, Keynote Speech.

[6] R. Resch, Our Solar Power Future: The US Industry Roadmap for 2030 and Beyond, 31st IEEE PVSC, 2005, Keynote Speech.

[7] B. O'Neill, Indium: Supply, Demand & Flat Panel Displays, Presented at Minor Metals 2004, London, June 2004.

[8] K. Zweibel, Environmental Aspects of PV Power Systems, Utrecht University, Netherlands, 1997.

[9] M. Spitzer, J.J. Loferski, J. Shewchun, Proc. of 14th IEEE PVSC, IEEE, New York, p.585 1980.

[10] O. Lundberg, M. Bodegard, J. Malmstrom, and L. Stolt, Progress in Photovoltaics: Research and Applications, 11, 77 2003.

[11] T. Negami, S. Nishiwaki, Y. Hashimoto, N. Kohara, Proc. of 2nd WCPEC, Vienna, 1181 1998.

[12] N. G. Dhere, S. R. Ghongadi, M. B. Pandit, A. H. Jahagirdar, D. Scheiman, CIGS2 Thin-Film Solar Cells on Flexible Foils for Space Power, Prog. Photovolt: Res. Appl. 2002, 10, p. 407–416.

[13] N. G. Dhere, V.S. Gade, A. A. Kadam, A. H. Jahagirdar, S. S. Kulkarni, S. M. Bet, Development of CIGS2 Thin Film Solar Cells, Materials Science and Engineering B, 116, 2004, pp. 303-109.

[14] N. G. Dhere, A. A. Kadam, S. S. Kulkarni, S. M. Bet A. H. Jahagirdar, Large Area CIGS2 Thin Film Solar Cells on Foils: Nucleus of a Pilot Plant, Solar Energy, 77, (2004), pp. 697-703.

[15] A. Rockett, "The effect of Na in polycrystalline and epitaxial single-crystal $CuIn_{1-x}Ga_xSe_2$" Thin Solid Films 480–481 (2005) pp. 2 –7

[16] J. E. Granata, J. R. Sites, J. Schmidt (Ed.), Proceedings of the Second World Conference on Photovoltaic Energy Conversion, Vienna, Austria, (1998), 604.

[17] CIS module pilot processing applying concurrent rapid selenization and sulfurization of large area thin film precursors. J. Palm , V. Probst , A. Brummer , W. Stetter , R. Tolle , T.P. Niesen , S. Visbeck , O. Hernandez , M. Wendl , H. Vogt , H. Calwer, B. Freienstein, F. Karg Thin Solid Films Volume 431-432, (2003),514-522.

[18] R. Klenk, S. Bakehe , R. Kaigawa , A. Neisser , J. Reiß , M. Ch. Lux-Steiner, Thin Solid Films 451 –452 (2004) 424–429.